Self-Assembly of Conjugated Polymers at the Air/Water Interface. Structure and Properties of Langmuir and Langmuir−Blodgett Films of Amphiphilic Regioregular Polythiophenes

Niels Reitzel,[†] Daniel R. Greve,[†] Kristian Kjaer,[‡] Paul B. Howes,[‡] Manikandan Jayaraman,[§] Steve Savoy,[||] Richard D. McCullough,[§] John T. McDevitt,[||] and Thomas Bjørnholm*,[†]

CISMI, Laboratory for Materials Science, Department of Chemistry, University of Copenhagen, Fruebjergvej 3, DK-2100 Copenhagen, Denmark, Condensed Matter Physics and Chemistry Department, RISØ National Laboratory, DK-4000 Roskilde, Denmark, Department of Chemistry, Carnegie Mellon University, Pittsburgh, Pennsylvania 15213, and Department of Chemistry and Biochemistry, University of Texas at Austin, Austin, Texas 78712

Received July 12, 1999

Abstract: This paper provides the first direct structural evidence describing conjugated polymer self-assembly at the air−water interface. Grazing-incidence X-ray diffraction (GIXD) and X-ray reflectivity measurements on a number of derivatives of amphiphilic regioregular polythiophenes (e.g., poly(3′-dodecyl-3-(2,5,8-trioxanonyl)-2′,5-bithiophene), polymer **1**) show that these conjugated polymers self-assemble as 2-dimensional polycrystalline monolayers at the air/water interface with the amphiphilic polymers preorganized into rigid boards standing edge-on on the water surface. The monolayer consists of highly ordered (∼70% crystalline) domains, with a centered rectangular unit cell having the polymer backbone along the *a*-axis and the thiophene π-stack along the *b* axis with a distance of 3.85−3.94 Å depending on the applied surface pressure. These domains are connected by soft, more disordered boundaries. This is evidenced by the macroscopic compressibility of the entire LB film ($C_{macro} \approx 4-7$ m/N) being one order of magnitude larger than the microscopic compressibility ($C_{micro} \approx 0.6$ m/N) of the polycrystalline domains. The alkyl chains in the 3-position of the thiophene rings are in a crystallographically disordered state due to their cross-sectional mismatch with the packing of the thiophenes. The importance of having the side chains coupled in a regioregular fashion to the 3-position of the thiophene rings is evidenced by a dramatic increase in the coherence length of the crystalline domains for highly regioregular samples (>95% head−tail couplings) as compared to less regioregularly coupled polymers (∼80% head−tail couplings). Transfer to solid support by the Langmuir−Blodgett technique induces an overall orientation of the domains in the film, giving rise to a dichroic ratio of up to 4. Reflection−absorption infrared spectroscopy (RAIRS) shows that the alkyl chains of transferred films are in an all-*trans* conformation with a locally ordered environment, having only few gauche defects.

Introduction

Synthesis and characterization of conjugated polymers has been a very active area of research since Little in 1964 suggested the possibility of superconductivity in these compounds.[1,2] Following these new ideas, high conductivity was measured in iodine-doped polyacetylene already in 1977, and a number of studies were subsequently dedicated to the mechanism of conductivity and other fundamental properties throughout the 1970s and 1980s.[3−6] Application of polyacetylene and other unsubstituted polymers initially developed[6] was difficult, however, because these polymers are insoluble in common organic solvents. This problem was overcome by tailoring precursor routes of conjugated polymers in a soluble form[7] or by adding flexible side chains to the backbone of the conjugated system.[8,9] Thin films of soluble polymers have subsequently been prepared by drop or spin casting, and they are presently being developed in technological applications as light-emitting diodes (LEDs),[10] sensors,[11,12] polymer electronics,[13] solar cells,[14−16] all-optical switching devices,[17,18] and possibly lasers.[19,20]

* To whom correspondence should be addressed. E-mail: tb@symbion.ki.ku.dk, http://www.bjornholm.dk.
[†] University of Copenhagen.
[‡] RISØ National Laboratory.
[§] Carnegie Mellon University.
[||] University of Texas at Austin.

(1) Little, W. A. *Phys. Rev. A* **1964**, *134*, 1416−1424.
(2) Little, W. A. *Sci. Am.* **1965**, *212*, 21−27.
(3) Chiang, C. K.; Fincher, C. R.; Park, Y. W.; Heeger, A. J.; Shirakawa, H.; Louis, E. J.; Gau, S. C.; MacDiarmid, A. G. *Phys. Rev. Lett.* **1977**, *39*, 1098−1101.
(4) Basescu, N.; Liu, Z.-X.; Moses, D.; Heeger, A. J.; Naarman, H.; Theophilou N. *Nature* **1987**, *327*, 403.
(5) Heeger, A. J. *Rev. Mod. Phys.* **1988**, *60*, 781−850.
(6) Skotheim, T. A.; Elsenbaumer, R. L.; Reynolds, J. R. *Handbook of Conducting Polymers*; Marcel Dekker: New York, 1998.
(7) Bradley, D. D. C. *J. Phys. D: Appl. Phys.* **1987**, *20*, 1389−1410.
(8) Wudl, F.; Allemand, P. M.; Srdanov, G.; Ni, Z.; McBranch, D. In *Materials for Nonlinear Optics: Chemical Perspectives*; Marder, S. R., Sohn, J. E., Stucky, G. D., Eds.; American Chemical Society: Washington, DC, 1991; p 683.
(9) McCullough, R. D. *Adv. Mater.* **1998**, *Vol 10, Iss 2*, 93.
(10) Burroughes, J. H.; Bradley, D. D. C.; Brown, A. R.; Marks, R. N.; MacKay, K.; Friend, R. H.; Burns, P. L.; Holmes, A. B. *Nature* **1990**, *347*(6293), 539−541.
(11) Bidan, G. *Sensor Actuator B Chem.* **1992**, *6*(1−3), 45−56.
(12) Dewit, M.; Vanneste, E.; Blockhuys, F.; Geise, H. J.; Mertens, R.; Nagels, P. *Synth. Met.* **1997**, *85*(1−3), 1303−1304.

10.1021/ja9924501 CCC: $19.00
Published on Web 06/02/2000

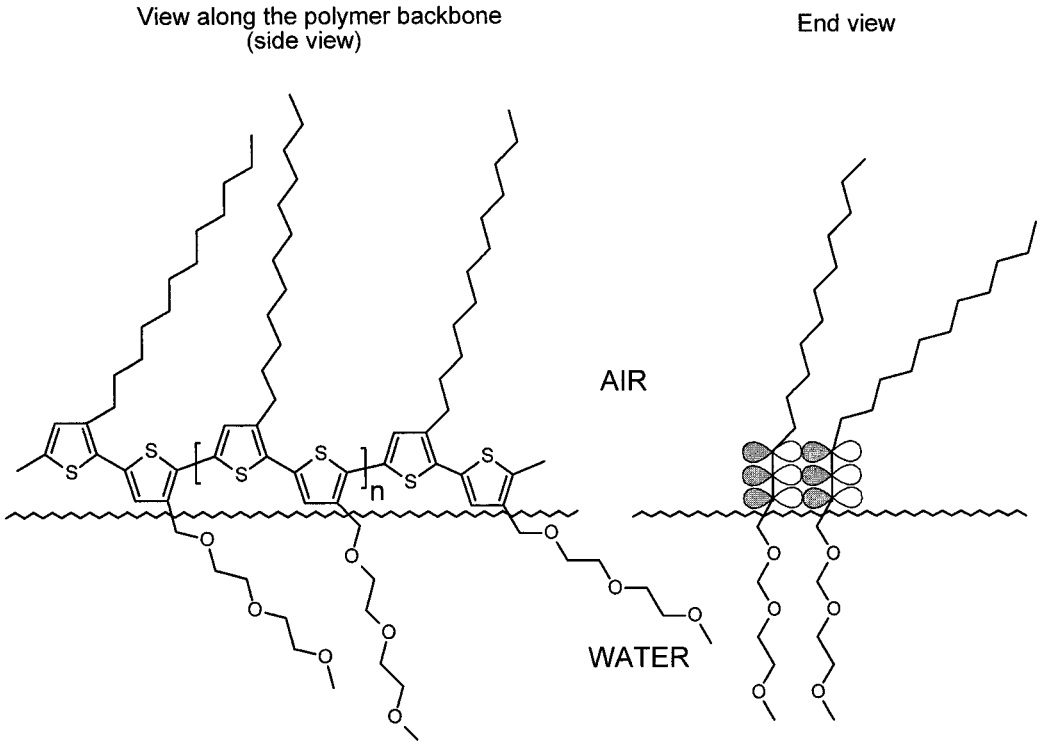

Figure 1. Left: single chain of regioregular amphiphilic polythiophene **1** at the air−water interface seen from the side. Right: schematic end view of two adjacent π-stacking polymer chains.

Since the electronic and optical properties of solution-processed conjugated polymer thin films are intimately connected to the packing motifs of the molecules in the films, it is of paramount importance to achieve control of the assembly process that take the polymers from a disordered state in solution into the semiordered solid state. The drive towards nanometer scale devices for future electronic applications further emphasizes the need of such nanoscale control.[21−27]

One way to study the self-assembly process of conjugated polymers is offered by the Langmuir−Blodgett (LB) technique,[28,29] which allows a self-assembled monolayer of amphiphilic molecules to be studied under well-defined experimental conditions. Originally, this technique was applied to simple molecular surfactants such as long chain alcohols and fatty acids,[28,29] and it was later developed to include more complex functionalized surfactants such as electron donors and acceptors,[27,30−36] surfactant conjugated polymers,[27,37−39] and rigid rod polymers substituted with alkyl chains.[40,41]

To further develop the processability of conjugated polymers with the aim of fabricating highly ordered nanoscale architectures, we have used the Langmuir−Blodgett technique to study and manipulate polythiophene. By design and synthesis of regioregular head-to-tail coupled amphiphilic polythiophene derivatives possessing a hydrophobic alkyl group at the 3-position of one thiophene ring and a hydrophilic group at the 3′-position of the adjacent thiophene ring (Figure 1) well-defined Langmuir−Blodgett films have been prepared and processed on the nanometer scale.[42,43] The nanoscale processability was

(13) Drury, C. J.; Mutsaers, C. M. J.; Hart, C. M.; Matters, M.; de Leeuw, D. M. *Appl. Phys. Lett.* **1998**, *73*, 108−110.
(14) Halls, J. J. M.; Pichler, K.; Friend, R. H.; Moratti, S. C.; Holmes, A. B. *Appl. Phys. Lett.* **1996**, *68*, 3120−3122.
(15) Halls, J. J. M.; Pichler, K.; Friend, R. H.; Moratti, S. C.; Holmes, A. B. *Synth. Met.* **1996**, *77*, 277−280.
(16) Curran, S.; Roth, S.; Davey, A. P.; Drury, A.; Blau, W. *Synth. Met.* **1996**, *83*, 239−243.
(17) Brédas, J. L.; Adant, C.; Tackx, P.; Persoons, A.; Pierce, B. M. *Chem. Rev.* **1994**, *94*, 243−278.
(18) Bjørnholm, T. *Isr. J. Chem.* **1996**, *36*, 349−356.
(19) Hide, F.; Diaz-Garcia, M. A.; Schwartz, B. J.; Andersson, M. R.; Pei, Q.; Heeger, A. J. *Science* **1996**, *273*, 1833−1836.
(20) Tessler, N.; Denton, G. J.; Friend, R. H. *Nature* **1996**, *382*, 695−697.
(21) *Ultimate Limits of Fabrication and Measurements*; NATO ASI Series E Vol. 292, Kluwer Academic Pub.: Dordrecht, 1995.
(22) Ball, P. *Made to measure*; Princeton University Press: Princeton, 1997.
(23) *Isr. J. Chem.* (Special issue on molecular machines) **1996**, *36*.
(24) *J. Mater. Chem.* (Special issue on molecular assemblies and nanochemistry) **1997**, *7*.
(25) *Nanostructures Based on Molecular Materials*; VCH: Weinheim, 1992.
(26) *Molecular Engineering for Advanced Materials*; NATO ASI Series C Vol. 456, Kluwer Academic Pub.: Dordrect, 1995.
(27) Bjørnholm, T.; Hassenkam, T.; Reitzel, N. *J. Mater. Chem.* **1999**, *9*, 1975−1990.
(28) Langmuir, I. *J. Am. Chem. Soc.* **1917**, *39*, 1848.
(29) Blodgett, K. B. *J. Am. Chem. Soc.* **1935**, *57*, 1007.
(30) Bryce, M. R.; Petty, M. C. *Nature* **1995**, *374*, 771.
(31) Vandevyver, M. *J. Chim. Phys.* **1988**, *85*, 1033−1037.
(32) Delhaès, P.; Yartsev, V. M. In *Spectroscopy of New Materials*; Clark, R. J. H., Hester, R. E., Eds.; John Wiley & Sons: New York, 1993; pp 199−289.
(33) Garnaes, J.; Larsen, N. B.; Bjørnholm, T.; Jørgensen, M.; Kjaer, K.; Als-Nielsen, J.; Joergensen, J. F.; Zasadzinski, J. A. *Science* **1994**, *264*, 1301−1304.
(34) Bjørnholm, T.; Geisler, T.; Larsen, J.; Jørgensen, M. *J. Chem. Soc., Chem. Commun.* **1992**, 815−17.
(35) Martin, A. S.; Sambles, J. R.; Ashwell, G. J. *Phys. Rev. Lett.* **1993**, *70*, 218.
(36) Metzger, R. M.; Chen, B.; Höpfner, U.; Lakshmikantham, M. V.; Vuillaume, D.; Kawai, T.; Wu, X. L.; Tachibana, H.; Hughes, T. V.; Sakurai, H.; Baldwin, J. W.; Hosch, C.; Cava, M. P.; Brehmer, L.; Ashwell, G. J. *J. Am. Chem. Soc.* **1997**, *119*, 10455−10466.
(37) Bolognesi, A.; Bajo, G.; Mazza, S. *Macromol. Symp.* **1997**, *118*, 657−662.
(38) Rulkens, R.; Wegner, G.; Enkelmann, V.; Schulze, M. *Ber. Bunsensges. Phys. Chem.* **1996**, *100*, 707−714.
(39) Bolognesi, A.; Bertini, F.; Bajo, G.; Provasoli, A.; Villa, D.; Ahumada, O. *Thin Solid Films* **1996**, *289*, 129−132.
(40) Orthmann, E.; Wegner, G. *Angew. Chem., Int. Ed. Engl.* **1986**, *25*, 114.
(41) Vahlenkamp, T.; Wegner, G. *Macromol. Chem. Phys.* **1994**, *195*, 1933.

demonstrated by the fabrication of a micro electronic circuit structure[42,44] and nanowires[43] of polythiophene using purely chemical self-assembly techniques.

Compared to other casting techniques the air/water interface offers some unique opportunities to study self-assembly processes. First, the "substrate" (water) is extremely well defined because it is flat and homogeneous, second, the effective dimensionality of the assembly process is reduced from 3 to 2 dimensions because molecules are confined to the water surface at which they are free to move only in the lateral direction, and third, recent developments of synchrotron sources, providing very intense X-rays, have allowed diffraction experiments to be performed directly on monomolecular films floating at the air/water interface.[45−50] This type of experiment allows the in-plane structure of the monolayer films to be elucidated for the first time. Once the films have been transferred to solid supports, local probe methods such as atomic force microscopy[51] may be used as well for studying the in-plane structure of the surface of the films.[27,33,52−57] In combination, these two methods allow the molecular structure of the individual amphiphiles to be related to the resulting in-plane structure of the films assembled at the air−water interface.

A very recent paper[58] on X-ray diffraction studies of spin cast poly(3-hexylthiophene) films has demonstrated that the structure and orientation of the crystalline domains in the films profoundly influence the charge carrier mobility. This is the first demonstration that the macroscopic electronic properties of these films may reflect both the orientation and structure of the crystallites embedded in the films as well as the domain boundaries connecting them. The result emphasizes the need to further understand and improve domain boundary formation as well as crystallite structure to optimize the electronic properties of these systems. Since the crystallite structure is the same in the spin cast polythiophene films and in the LB-films described here, the latter can serve as a sliced 2-dimensional model systems in which the structure and domain boundary formation can be studied in a direct and unambiguous way.

Here we present the structural and basic physical properties of a number of amphiphilic polymeric and monomeric thiophene derivatives studied both as monomolecular layers on water (Langmuir films) and as Langmuir−Blodgett films transferred to solid supports. The structural and physical data for these molecules are discussed with special emphasis on the relation between molecular design and the resulting self-assembled structures.

Table 1. Molecules Included in the Present Study

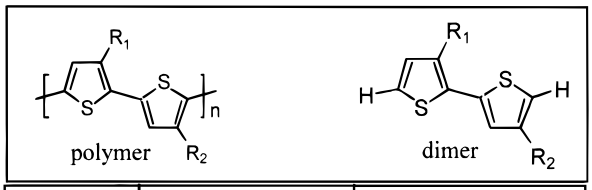

#	R_1	R_2
1	$C_{12}H_{25}$ -	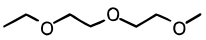
2 dimer		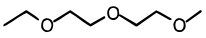
3		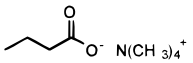
4		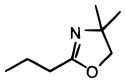
5		$C_{12}H_{25}$ -
6	$C_{16}H_{33}$ -	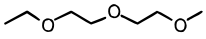
7	$C_{18}H_{37}$ -	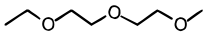
8	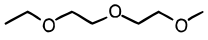	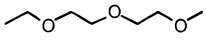

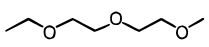 = MEEM

Experimental Section

The synthesis of compounds **1**−**5** (Table 1) was reported previously,[42,59,60] and compounds **6**−**8** were synthesized using the same procedures.[42] The structure of all the molecules used was characterized by ^{1}H and ^{13}C NMR. The polymeric derivatives were furthermore analyzed by size-exclusion chromatography analysis (SEC) using polystyrene standards.[61,62]

Chloroform solutions of the amphiphilic polythiophene derivatives (∼1 mg/mL) were spread onto the Milli-Q purified water subphase (18.2 MΩcm) of a LB trough (KSV5000 or Lauda) which was

(42) Bjørnholm, T.; Greve, D. R.; Reitzel, N.; Hassenkam, T.; Kjaer, K.; Howes, P. B.; Larsen, N. B.; Bøgelund, J.; Jayaraman, M.; Ewbank, P. C.; McCullough, R. D. *J. Am. Chem. Soc.* **1998**, *120*, 7643−7644.
(43) Bjørnholm, T.; Hassenkam, T.; Greve, D. R.; McCullough, R. D.; Jayaraman, M.; Savoy, M. S.; Jones, C. E.; McDevitt, J. T. *Adv. Mater.* **1999**, *11*, 1218−1221.
(44) Greve, D. R.; Reitzel, N.; Hassenkam, T.; Bøgelund, J.; Kjaer, K.; Howes, P. B.; Larsen, N. B.; Jayaraman, M.; McCullough, R. D.; Bjørnholm, T. *Synth. Met.* **1999**, *102*, 1502−1505.
(45) Als-Nielsen, J.; Kjaer, K. In *NATO Advanced Study Institute on phase transitions in soft condensed matter*, Geilo, 4−14 Apr 1989; Riste, T., Sherrington, D., Eds.; Plenum Press: New York, 1989; pp 113−138.
(46) Kjaer, K.; Als-Nielsen, J.; Helm, C. A.; Laxhuber, L. A.; Möhwald, H. *Phys. Rev. Lett.* **1987**, *58*, 2224−2227.
(47) Kjaer, K. *Physica B* **1994**, *198*, 100−109.
(48) Als-Nielsen, J.; Jacquemain, D.; Kjaer, K.; Leveiller, F.; Lahav, M.; Leiserowitz, L. *Phys. Rep.* **1994**, *246*, 251−313.
(49) Als-Nielsen, J.; Möhwald, H. *Handb. Synchrotron Radiat.* **1991**, *4*, 3−53.
(50) Weissbuch, I.; Popovitz-Biro, R.; Lahav, M.; Leiserowitz, L.; Kjaer, K.; Als-Nielsen, J. *Adv. Chem. Phys.* **1997**, *102*, 39−120.
(51) Binnig, G.; Quate, C. F.; Gerber, C. *Phys. Rev. Lett.* **1986**, *56*, 930.
(52) Garnaes, J.; Schwartz, D. K.; Viswanathan, R.; Zasadzinski, J. A. N. *Nature* **1992**, *357*, 54.
(53) Schwartz, D. K.; Garnaes, J.; Viswanathan, R.; Zasadzinski, J. A. N. *Science* **1992**, *257*, 508.
(54) Maliszewskyj, N. C.; Heiney, P. A.; Josefowicz, J. Y.; Plesnivy, T.; Ringsdorf, H.; Schuhmacher, P. *Langmuir* **1995**, *11*, 1666−1674.
(55) Henderson, P.; Beyer, D.; Jonas, U.; Karthaus, O.; Ringsdorf, H.; Heiney, P. A.; Maliszewskyj, N. C.; Ghosh, S. S.; Mindyuk, O. Y.; Josefowicz, J. Y. *J. Am. Chem. Soc.* **1997**, *119*, 4740−4748.
(56) Riul, A.; Mattoso, L. H. C.; Telles, G. D.; Herrmann, P. S. P.; Colnago, L. A.; Parizotto, N. A.; Baranauskas, V.; Faria, R. M.; Oliveira, O. N., Jr. *Thin Solid Films* **1996**, *284*−*285*, 177−180.
(57) Matsuzaki, H.; Ogasawara, K.; Ishiguro, T.; Nogami, Y.; Taoda, M.; Tachibana, H.; Matsumoto, M.; Nakamura, T. *Synth. Met.* **1995**, *74*, 251−255.
(58) Sirringhaus, H.; Brown, P. J.; Friend, R. H.; Nielsen, M. M.; Bechgaard, K.; Langeveld-Voss, B. M. W.; Spiering, A. J. H.; Janssen, R. A. J.; Meijer, E. W.; Herwig, P.; de Leeuw, D. M. *Nature* **1999**, *401*, 685−688.
(59) McCullough, R. D.; Ewbank, P. C.; Loewe, R. S. *J. Am. Chem. Soc.* **1997**, *119*, 633.
(60) McCullough, R. D.; Lowe, R. D.; Jayaraman, M.; Anderson, D. L. *J. Org. Chem.* **1993**, *58*, 904.
(61) Yay, W. W.; Kirkland, J. J.; Bly, D. D. *Modern Size-Exclusion Liquid Chromatography*; John Wiley & Sons: New York, 1979.
(62) Vanhee, S.; Rulkens, R.; Lehmann, U.; Schulze, M.; Köhler, W.; Wegner, G. *Macromolecules* **1996**, *29*, 5136−5142.

subsequently used for LB-film preparation. To achieve hydrophilic surfaces, substrates of glass, quartz, and silicon were cleaned in boiling piraña solution (H_2O_2/H_2SO_4 (1:3)) prior to use. Gold film samples were deposited as 2000 Å thick layers, prepared by resistive evaporation (Edwards auto 306 metal evaporator with cryodrive pump) onto a 50 Å Cr adhesion layer as described earlier.[63] In some cases, the gold films were treated with an ethanolic solution of mercaptoacetic acid to increase the hydrophilicity of the gold surface. Absorption in the UV−vis region was measured on a Perkin-Elmer Lambda 9 spectrometer on films transferred to glass or quartz (transfer ratio of 1 ± 0.1). The dichroic ratio was measured using a commercial Perkin-Elmer polarizer-insert in the Lambda 9 spectrometer. Reflection−absorption infrared spectroscopy (RAIRS) was recorded on a Nicolet 550 Fourier transform spectrometer as described in reference.[63] AFM measurements were performed on a Nanoscope III Digital Instruments microscope using standard silicon nitride tips in contact mode. Two X-ray techniques were used: Specular reflectivity measurements and Grazing-incidence X-ray diffraction (GIXD). The measurements were performed on the liquid surface diffractometer at the X-ray undulator beamline BW1 at the synchrotron facility HASYLAB at DESY in Hamburg, Germany. A Langmuir trough, placed in a sealed, He-filled, thermostated canister and provided with a Wilhelmy balance for monitoring the surface pressure, was used on the diffractometer. The setups are thoroughly explained elsewhere.[48−50,64] The X-ray wavelengths used in different runs were 1.448 Å and 1.3037 Å, monochromated by Bragg reflection by a Be(002) crystal. For the GIXD, the angle of incidence (α_i) was slightly below the critical angle (α_c) for total reflection ($\alpha_i = 0.85\alpha_c$), thus increasing the surface sensitivity by minimizing the penetration depth of the incident X-rays into the water subphase. The horizontal scattering angle ($2\theta_{xy}$) was resolved with a Soller collimator, while the vertical exit angle (α_f) of the diffracted radiation was detected with a Position sensitive detector (PSD), detecting diffracted photons over a range $0.0 \le Q_z \le 0.9$ Å^{-1} (Q_z is the vertical component of the scattering vector **Q**: $Q_z = (2\pi/\lambda)\sin\alpha_f$).

Results

The molecules encountered in the present study are shown in Table 1, and a typical example is illustrated in Figure 1. The physical and chemical data are summarized in Tables 2−5.

1. Langmuir Films. Chloroform solutions of the polythiophene derivatives **1**−**4** and **6**−**8** are readily spread onto the water surface of a Langmuir trough. The pressure−area isotherm for a representative derivative, **1**, is shown in Figure 2A. The compression proceeds smoothly until the film collapses at an area corresponding to ∼29 Å^2 per bithiophene unit. This collapse area agrees with the area per repeat unit estimated from molecular models of the repeat unit having the plane of the thiophene unit vertical to the water surface (Figure 1). This picture is confirmed by X-ray studies as described in the following sections. The collapse areas of the other amphiphilic polymers in Table 1 are comparable to **1**, suggesting that all the amphiphilic polythiophenes investigated here form monolayer arrangements roughly similar to that represented in detail here for **1**. The nonamphiphilic poly(3-dodecylthiophene) **5** does not spread into a monolayer at the water surface as seen in Figure 2A. The all-polar homo-polymer **8** does form a crystalline monolayer which, however, has a $\lambda_{max} \approx 480-510$ nm indicating a less conjugated structure than for the amphiphilic derivatives. The results on the homo-polymers **5** and **8** corroborate previous studies of nonamphiphilic polythiophene derivatives.[39,65−71]

Table 2. Summary of Molecular Weight Distributions and Crystallographic Data

compd	⟨MW⟩ (g/mol)[a]	PDI[a]	% RR-HT[b]	λ_{max}[c] (nm)	d_{02}[d] (Å)	L[e] (Å)
1	15 300	1.3	95	544	3.82−3.85	∼50
1	24 600	1.3	95	544	3.88	∼50
2	466	1		299		< 10
3	7000	4	98	510		
4	7000	4	98	525		
5	20 000	1.5	98	550		
6-RR	17 300	1.8	95	545	∼3.8	∼40
6-RIR	11 125	1.8	80	520	∼3.9	∼27
7	54 000	3.6	95	510		
8	46 100	1.5	98	510		

[a] PDI (poly dispersity index) from analysis of SEC (size exclusion chromatograpy) data using polystyrene standards. These values are normally 30−40% higher than those obtained by integration of the NMR signal from of end-group protons.[94] [b] The head−tail ratio is estimated by ^{1}H NMR as the ratio between the integrated signals from HT and non-HT protons observed in the aromatic and benzylic regions, in analogy to poly-3-alkylthiophenes.[60] [c] Measured on solution cast films on glass. [d] Estimated from the position of the diffraction peaks of compressed monolayer (30 mN/m). [e] Coherence length estimated from the full width half-maximum of d_{02} peaks measured by X-ray diffraction using the Scherrer formula: $L \approx 2\pi 0.9/\text{fwhm}(Q_{xy})$.

2. Grazing-Incidence X-ray Diffraction (GIXD) from Langmuir Films. The in-plane structure of a Langmuir monolayer of **1** compressed to a surface pressure of 30 mN/m has been elucidated by synchrotron X-ray diffraction. Figure 2C shows the observed Bragg reflections from this monolayer on water vs the in-plane component Q_{xy} of the scattering vector. A superposition of three peaks corresponding to interplanar spacings of 3.84 and 5.42 Å for the narrow peaks and ∼4.6 Å for the broad peak is observed on top of the scattering measured for a pure water surface, which has been subtracted from the data. Decomposition of the intensity profile into three peaks allows the coherence length (L) of the scattering domains to be estimated to be $L \approx 50$ Å for the two narrow peaks and $L \approx 10$ Å for the broad peak using the Scherrer formula ($L = 2\pi$*0.9/fwhm(Q_{xy})).[72] The intense narrow peak corresponds to the π-stacking distance of polythiophene.[73] With respect to the centered cell shown in Figure 2B, this is the {02} reflection ($d_{02} = 3.84 \pm 0.02$ Å $= (1/2)$*$|b|$). The position of the weak {11} peak in this cell yields $d_{11} = 5.42 \pm 0.05$ Å. Assuming a rectangular cell ($\gamma = 90°$), the d_{02} and d_{11} values lead to a unit cell vector **a** = 7.66 Å, representing the repeat unit distance along the polymer backbone. Within experimental error, this value is in agreement with computer modeling using standard bond lengths and angles (**a** = 7.66−7.85 Å).[74] Other indirect sources of the polymer repeat distance provide values between 7.6 and 7.9 Å.[75−77] Allowing this uncertainty in **a** yields $\Delta\gamma = \pm 3°$. The {20} peak corresponding to the polymer repeat distance is then coincident with the {02} peak ($d_{20} =$ 3.83 Å). However, in all the model calculations performed (cf.

(63) Ritchie, J. E.; Wells, C. A.; Zhou, J.-P.; Zhao, J.; McDevitt, J. T.; Ankrum, C. R.; Jean, L.; Kanis, D. R. *J. Am. Chem. Soc.* **1998**, *120*, 2733−2745.
(64) Leveiller, F.; Jacquemain, D.; Leiserowitz, L.; Kjaer, K.; Als-Nielsen, J. *J. Phys. Chem.* **1992**, *96*(25), 10380−10389.
(65) Fou, A. C.; Rubner, M. F. *Macromolecules* **1995**, *28*, 7115.
(66) Ferreirra, M.; Rubner, M. F. *Macromolecules* **1995**, *28*, 7107.
(67) Ahlskog, M.; Paloheimo, J.; Stubb, H.; Dyreklev, P.; Fahlman, M.; Inganäs, O. *J. Appl. Phys.* **1994**, *76*, 893.
(68) Ochiai, K.; Rikukawa, M.; Sanui, K. *Chem. Commun.* **1999**, 867−868.
(69) Cirak, J.; Tomecik, P.; Cerven, I.; Cik, G.; Vegh, D. *Supramol. Sci.* **1997**, *4*, 539−542.
(70) Liu, Y. Q.; Xu, Y.; Zhu, D. B. *Synth. Met.* **1997**, *84*, 197−198.
(71) Schottland, P.; Fichet, O.; Teyssie, D.; Chevrot, C. *Synth. Met.* **1999**, *101*, 7−8.
(72) Guinier, A. *X-ray diffraction* **1963**, Chapter 5.5.
(73) Prosa, T. J.; Winokur, M. J.; McCullough, R. D. *Macromolecules* **1996**, *29*, 3654−3656.
(74) Allinger, N. L. *J. Am. Chem. Soc.* **1977**, *99*, 8127−8134.
(75) Prosa, T. J.; Winokur, M. J.; Moultan, J.; Smith, P.; Heeger, A. J. *Macromolecules* **1992**, *25*, 4364−4372.

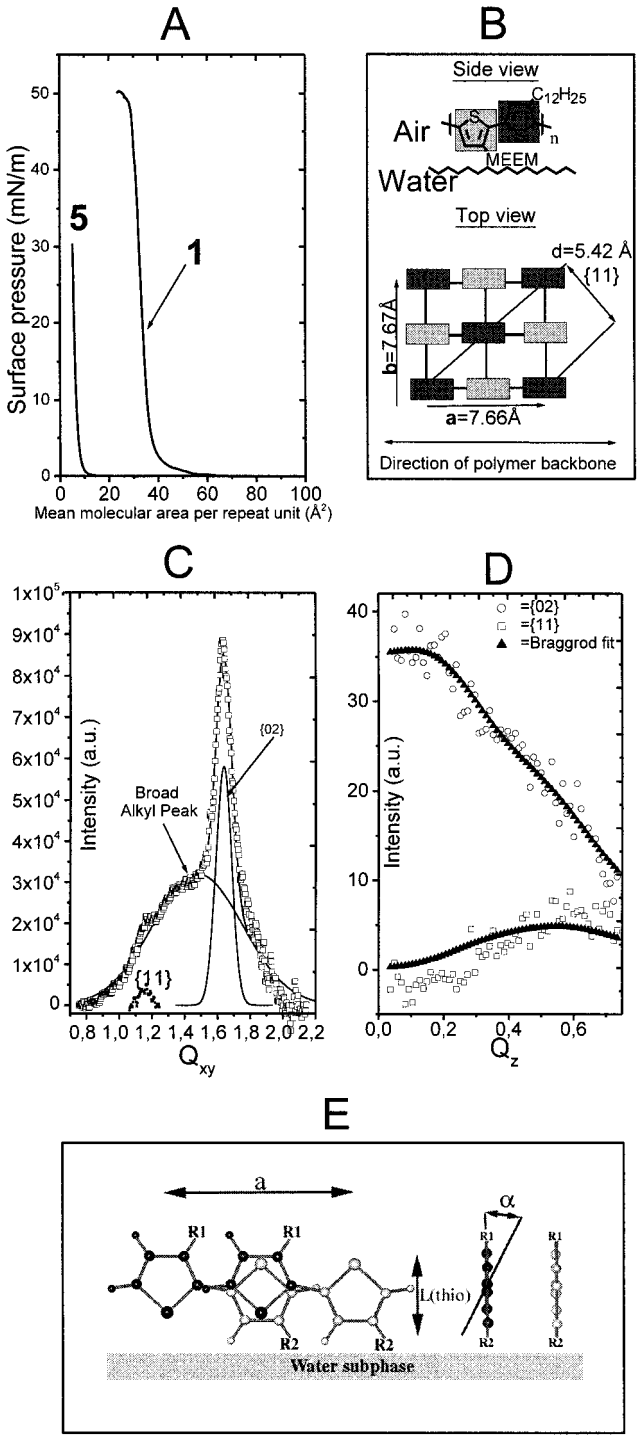

Figure 2. A: Compression isotherms of amphiphilic polymer **1** forming a stable Langmuir film with a collapse area of ~29 Å^2 and the nonamphiphilic polymer **5**, which does not form a monolayer. B: Summary of the 2-D crystal structure of a Langmuir film of polymer **1** elucidated by synchrotron GIXD. A centered rectangular unit cell is formed as shown with the hydrophilic-substituted thiophene moieties in light gray color and the hydrophobic-substituted thiophene moieties colored in dark gray. C: Bragg peak projection of the diffracted signal with three features: the small {11} peak and the sharp, intense {02} peak originating from the π-stacked thiophenes, and a broad peak originating from a disordered alkyl chain layer. D: Bragg rod profile of the {02} (circles) and {11} (squares) peaks with the corresponding Bragg rod fits (triangles) described in the text. E: Side view (left) and end view (right) of two thiophene dimers having the same color code as B.

below) the contribution from the {20} reflection is negligible in comparison with the {02} contribution. Hence, for convenience, the intense narrow peak will be referred to as the {02} peak in the following. The peak which is broad in Q_{xy} (Figure 2C) is assumed to be due to incoherent scattering from the alkyl chains. This is consistent with our observation of an increased intensity of this peak for a compound with an increased alkyl chain length as exemplified by **6** (cf. Table 1 and Figures 2C and 3B).

Resolving the scattering in the Q_z direction and integrating over Q_{xy} across each peak yields the so-called Bragg rods $I(Q_z)$.[47,48] Figure 2D shows a fit to the $I(Q_z)$ data of the {02} and the {11} reflections based on a structural model as depicted in Figure 2B, where the alkyl chains were omitted. In fitting the Bragg rods (Figure 2D), the centered rectangular unit cell shown in Figure 2B was used. It was found that the best fit to the Bragg rod data could be obtained by only taking into account the scattering from the polythiophene backbone having the two closest methylene groups attached (an alkyl methylene and a MEEM methylene (MEEM is the 2,5,8-trioxanonyl side-group)).[78] The remaining parts of the substituent chains (MEEM and alkyl) are thus assumed to be incoherent, i.e., to have large mean-square displacements (in accordance with the RAIRS data presented below). For the well-ordered thiophene part of the molecule, the out-of-plane thermal displacement is 0.45 Å rms. and the in-plane displacement is 0.98 Å rms. The best fit was obtained with the plane of the thiophene rings being normal to the water surface with an uncertainty (α in Figure 2E) of $\pm 10°$.[78] In summary, these data provide the most accurate estimate of the local packing of adjacent thiophene units in regioregular poly(3-alkylthiophene) derivatives reported to date.

An estimate of the degree of crystallinity of the monolayer was made by comparing the scattering intensity from the {02} and {11} reflections originating from thiophene moieties to the intensity arising from the disordered side groups (broad peak in Figure 2C). The estimate is based on the assumption that the broad side group peak serves as an internal reference for the scattered intensity, because the scattering intensity from the incoherent side groups is independent of the degree of crystallinity in the thiophene moieties. By comparing the integrated experimental values to the calculated scattering intensity of the thiophene and side group moieties respectively, we estimate that ~70% of the thiophene moieties are in a crystalline state.

GIXD studies were also made on dimer **2**, 80% and 95% regioregular **6**, and on 95% regioregular **7** (Tables 1−3). The results are summarized in Figure 3 showing the compression isotherms (top) and the observed diffraction from Langmuir films (bottom).[79] The compression isotherm of dimer **2** (Figure 3A top) shows a phase transition at an area of ~42 Å^2. For this compound, GIXD measurements were made on each of the phases at the pressures $\pi(1) = 7.6$ mN/m and $\pi(2) = 24.6$ mN/m, marked with crosses. The diffraction patterns (Figure 3A, bottom) show only scattering from amorphous phases, indicating

(76) Corish, J.; Morton-Blake, D. A.; Beniere, F.; Lantoine, M. *J. Chem. Soc., Faraday Trans.* **1996**, *92*, 671−677.

(77) Chen, S. A.; Lee, S. J. *Synth. Met.* **1995**, *72*, 253−260.

(78) Fitting the Bragg rods was done systematically by varying the position of the atoms in the unit cell, and the number of methylene groups from the side chains contributing to the coherent scattering. The goodness of the fits was evaluated by normalized χ^2 values (e.g., tilting the bithiophene having two methylene groups resulted in the following (tilt angle; χ^2 value)-pairs: (0; 4.4), (5; 4.7), (10; 5.9), (15; 8.0), where 0° refers to the bithiophene being orthogonal to the subphase).

(79) The Q_{xy}-GID scans are not Q_z resolved and have a lower signal-to-noise ratio than those of Figure 2; hence, small features such as the {11} peak are not resolved.

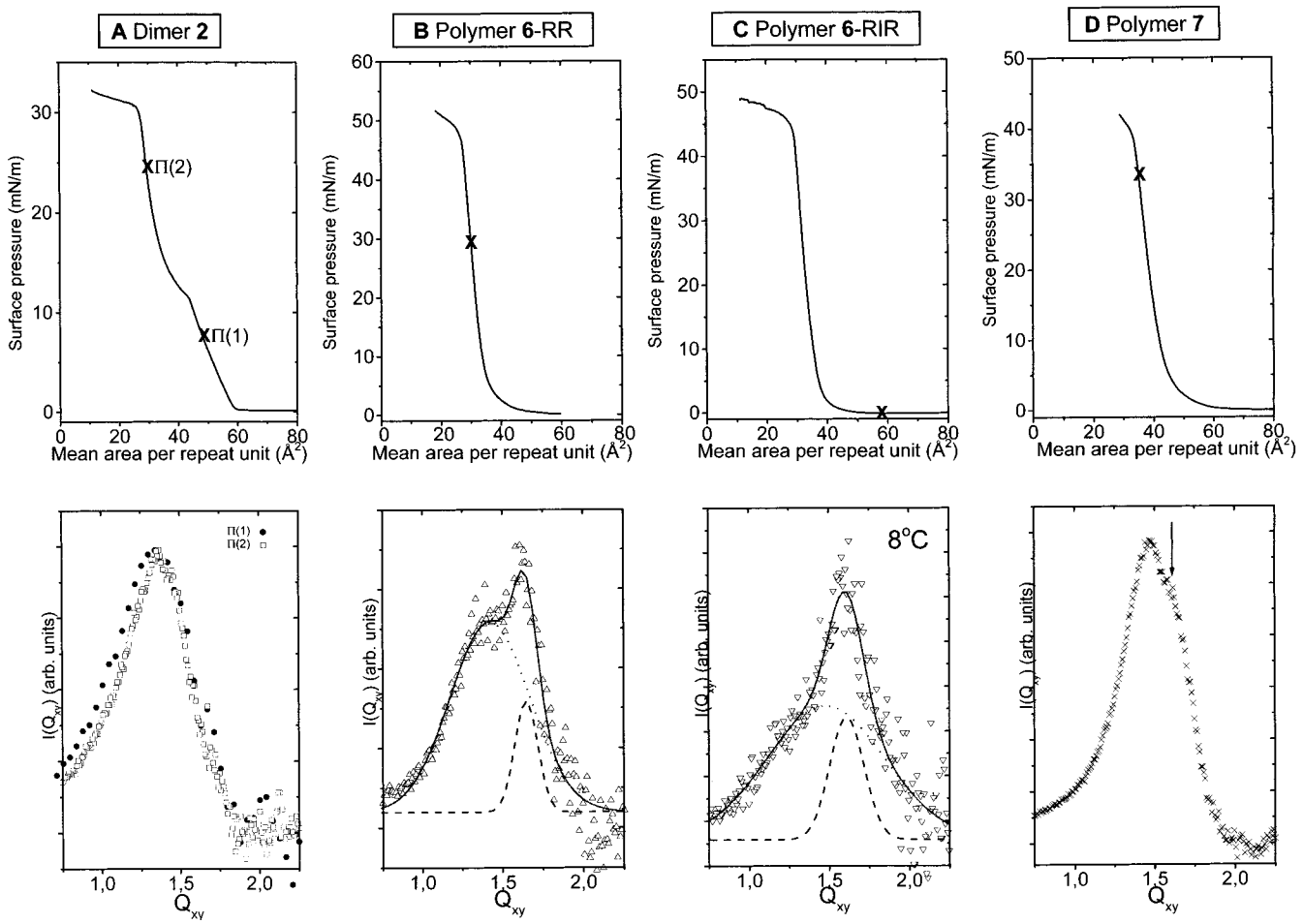

Figure 3. Compression isotherms (top) and GIXD results (bottom) of dimer **2** (A), regioregular polymer **6** (B), regioirregular polymer **6** (C), and polymer **7** (D). The crosses on the compression isotherm mark the pressures at which the GIXD measurements were performed.

Table 3. Summary of Compressibility Data of Langmuir Films

compd	MW (g/mol)	PDI	macroscopic compressibility (m/N)	microscopic compressibility (m/N)	% RR-HT
1	15 300	1.3	3.7	0.58	95
1	24 600	1.3	3.7	0.57	95
6-RR	17 300	1.8	5.4		98
6-RIR	11 125	1.8	5.2		80
7	54 000	3.6	7.2		95

that dimer **2** does not organize as a 2D-crystalline Langmuir film.

The diffraction from 95% regioregular polymer **6** (Figure 3B, taken at 20 °C and a surface pressure of 29 mN/m) shows two features: a broad peak (from an amorphous alkyl layer) and a narrow peak (at $Q_{xy} = 1.64$) corresponding to a π-stacking distance of 3.85 ± 0.05 Å. From the width of the Gaussian fit to this peak (dashed), a coherence length of 40 Å (corresponding to ~10 π-stacks) was calculated by the Scherrer formula. The diffraction from the regioirregular polymer **6** was recorded at very low surface pressure. Compression of this regioirregular sample only decreased the diffracted intensity. Furthermore, at room temperature, only broad scattering from amorphous phases was seen. The diffraction pattern shown in Figure 3C was obtained on cooling to 8 °C. The diffracted signal was fitted by two Gaussians. The narrow peak, corresponding to the π-stacking distance, has a repeat distance $d = 3.90 \pm 0.05$ Å, and from the peak width, a coherence length of 27 Å (corresponding to ~7 crystalline ordered π-stacks) was deduced. For a compressed Langmuir film of the C-18 substituted amphiphilic polymer **7** (at 21 °C) the diffraction signal is markedly different (Figure 3D). Only the shoulder at $Q_{xy} \approx 1.61$ (corresponding to $d \approx 3.8$ Å), marked by an arrow in Figure 3D (bottom), is presumably due to the π-stacking. The peak with $d \approx 4.6$ Å is sharper than in Figure 3B,C, presumably because a regular packing of the alkyl chains is beginning to dominate the overall crystal structure. The results are summarized in Table 2.

3. Relation between the in-Plane Structure and Surface Pressure (Compressibility). Figure 4 shows the results of Q_{xy}-GIXD scans on monolayers of two different fractions of polymer **1** with ⟨Mw⟩ = 15 300 g/mol and ⟨Mw⟩ = 24 600 g/mol, respectively, as a function of the area of the polymer repeat unit (i.e., a thiophene dimer) projected onto the water surface. After background subtraction and Lorentz, polarization, and area corrections, the scans have been fitted by two Gaussians as exemplified in Figure 3. On the basis of these Gaussian fits to the {02} reflection, the π-stacking distance (d_{02}), and the diffraction intensity, I, have been plotted versus the area per repeat unit in the polymer (Figure 4B,C). In addition, the surface pressure has been plotted as function of the crystallographic repeat unit area in Figure 4D.

Figure 4A shows compression isotherms with crosses indicating where the GIXD measurements were performed. Figure 4B shows the interplanar spacing (d_{02}). It is seen that crystalline domains form, even when the Langmuir layer is uncompressed; i.e., the molecules self-assemble on the water surface. When the domains are pressed together to form a monolayer, a decrease in the π-stacking distance (d_{02}) of less than 0.1 Å is observed. It is also seen that the $\pi-\pi$ distance of the high

Table 4. Summary of X-ray Reflectivity Data[a]

compd	L_{alkyl} (Å)	N_{alkyl}	L_{thio} (Å)	N_{thio}	L_{polar} (Å)	N_{polar}	σ (Å)	no. of H_2O	π (mN/m)	A (Å^2) (fit (iso))
1	11.2	97	4.7	82	8	93	3.3	2	30	32 (33)
2	9.2	97	3.5	84	6.0	89	3.4	2	7.8	43 (47)
2	13.6	97	5.6	92	8.8	97	4.3	3	24.3	31 (30)
6	14.5	129	4.7	82	7.7	91	4.3	2	30	32 (31)

[a] MEEM: 73 electrons.

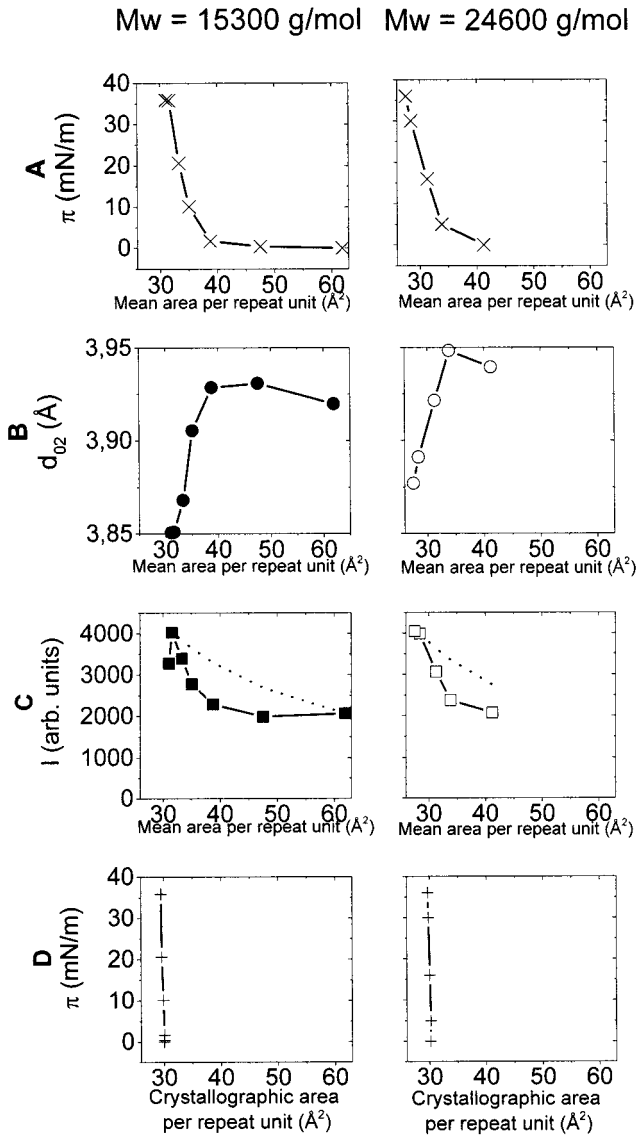

Figure 4. Results from GIXD measurements on two different fractions of polymer **1** having different mean molecular weights (fractionated by SEC). A: The compression isotherms with crosses indicating where the GIXD measurements were performed. B: π-Stacking distance of the thiophene units as a function of the mean molecular area. C: Measured intensity (squares) and calculated intensity (dashed line) of the {02} Bragg peak (the area under the peak). D: Surface pressure as function of the crystallographic area per repeat unit, obtained as $d_{02} \times a$.

molecular weight fraction is larger than that of the low molecular weight fraction, indicating a better π-stacking of polymers having shorter polymer chain lengths. Figure 4C shows the area under the {02} Bragg peaks, which is proportional to the scattering intensity and, hence, the amount of crystalline domains floating on the water surface. The calculated intensity is expected to be inversely proportional to the mean area per molecule, because an increasing number of polymer domains are pushed into the X-ray beam footprint on the water surface as the monolayer is compressed. This hyperbolic relationship between intensity and area is shown by the dotted line in Figure 4C, where the calculated intensity has been normalized to the measured data at the point just before collapse. The fact that the measured diffracted intensity is lower than the calculated intensity during compression is interpreted as being due to mechanical stress during the compression leading to a breakup of the crystalline domains originally formed after the spreading process.

Figure 4D shows the increase in surface pressure as a function of the crystallographic area per repeat unit, derived from the d_{02} spacing ($A_{cryst} = d_{02}$ 7.66 Å). A change in d_{02} from 3.92 to 3.85 Å in the π-stacking distance is observed for the low M_w fraction when the pressure is changed from 0 to 35 mN/m. The change is equivalent to a 2% change in the unit cell area.[80]

The knowledge of the crystallographic unit cell parameters, the mean area per molecule of the compression isotherm, and the applied surface pressure offers the possibility of comparing the standard macroscopic 2-D compressibility inferred from the compression isotherms, with the microscopic compressibility obtained from diffraction. The 2-D compressibility (C) is defined in eq 1.[81,82]

$$C = -(1/A)(\partial A/\partial \pi)_T \qquad (1)$$

For evaluation of the macroscopic compressibility, A in eq 1 is the mean area per molecule. Hence, it is found from the negative slope of the compression isotherm (Figure 4A). This measurement is an average over the mechanical properties of the Langmuir film, taking into account both the crystalline and the amorphous parts.

The microscopic compressibility, on the other hand, pinpoints the mechanical properties of the crystalline areas (which gives rise to Bragg diffraction). It is calculated by inserting A_{cryst} into eq 1, i.e., from the negative slope of Figure 4D. The compressibility data are summarized in Table 3.

As seen, the microscopic compressibility is an order of magnitude smaller than the macroscopic compressibility in agreement with the notion that the domain boundaries are disordered and soft, while the crystallites are hard. In consequence, the data show that during compression of the monolayer, mainly the amorphous domain boundaries are affected while the π-stacks in the interior of the self-assembled crystalline domains remain almost unchanged.

4. X-Reflectivity from Langmuir Films. X-ray reflectivity studies have been used to provide the electron density profile perpendicular to the water surface of Langmuir films of representative examples of the derivatives under consideration. The top row of Figure 5A−D shows the measured reflectivity normalized to the Fresnel reflectivity, R/R_F (squares), and the best fit to the data (solid line). The electron density profile

(80) The compression of the backbone is assumed negligible. Application of Hookes law, with a force constant of ~500 N/m (a typical value of a chemical bond[74]) and an applied surface pressure of 0.040 N/m gives $\Delta \mathbf{a} = 0.002$ Å.

(81) Gaines, G. L. *Insoluble Monolayers at Liquid−Gas Interfaces*; Interscience: New York, 1966.

(82) Behroozi, F. *Langmuir* **1996**, *12*, 2289−2291.

Table 5. Summary of RAIRS Data[a]

compd	MW (g/mol)	$\nu_{asym}(CH_2)$ (cm^{-1})	$fwhm_{asym}(CH_2)$ (cm^{-1})	$\nu_{asym}(CH_3)$ (cm^{-1})	$fwhm_{asym}(CH_3)$ (cm^{-1})
1	13 000	2920	13	2966	13
1	22 000	2924	21	2964	15
solid PE		2918	14−18		
liquid PE		2924	30		

[a] PE: polyethylene.

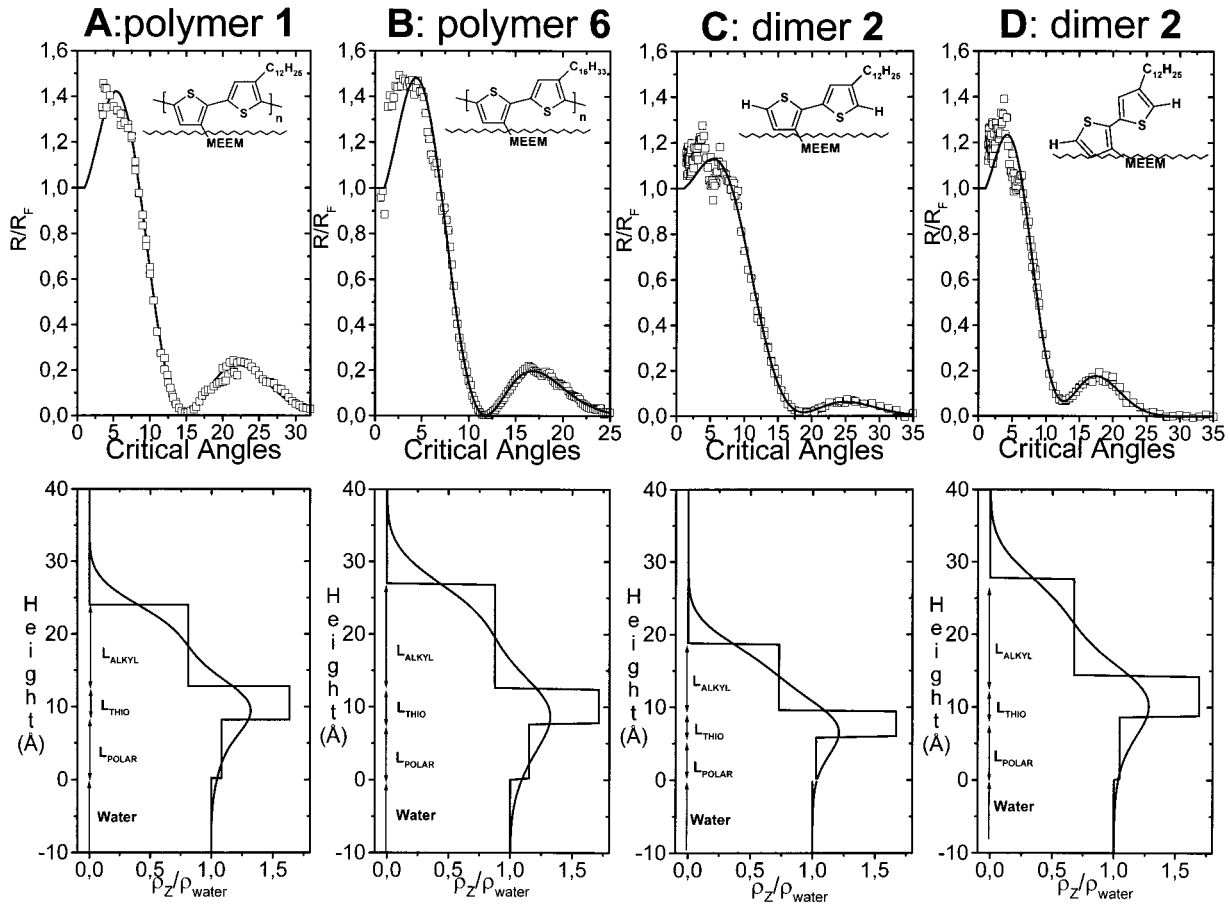

Figure 5. Synchrotron X-ray reflectivity measurements of polymer **1** (A), polymer **6** (B), dimer **2** (at a surface pressure $\pi = 8$ mN/m, C) and dimer **2** (at a surface pressure $\pi = 25$ mN/m, D). The top row shows the experimental data (squares) as a function of the angle of incidence normalized to the critical angle for total reflection from a clean water surface. The solid line is a three-box model fit (see text) to the data as shown in the bottom row. The three boxes represent the alkyl chain, the thiophene backbone, and the hydrated polar MEEM group layers. The height above the water surface is plotted as a function of the electron density of the layers (ρ_z) normalized to the electron density of pure water (ρ_{water}). The boxes have been smeared with a thermal displacement factor, giving the smooth line (Table 4).

deduced by the least-squares fitting is shown in the bottom of Figure 5.

The electron density profile[45,47,48,83] of a compressed Langmuir film ($\pi = 30$ mN/m) of polymer **1** is found to be consistent with the predicted electron density of stacked, upright polythiophenes amphiphilically ordered at the air−water interface (cf. Figures 1 and 2B) having tilted alkyl chains and hydrated polar substituents, as evidenced by the excellent fit of the experimental data by such a profile (Figure 5A). As seen from Figure 5B, Langmuir films of **6**, having four extra carbon atoms in the alkyl chain, are similar to monolayers of **1** except for the extension of the alkyl chain.

The reflectivity of dimer **2** shown in Figure 5C,D is considerably different from the polymeric derivatives. The reflectivity data explain the phase transition, which was seen by the kink in the compression isotherm (Figure 3A, top): In the low-pressure phase (Figure 5C), the thiophene dimer is lying on the water subphase, while, in the high-pressure phase, the thiophene bearing the hydrophobic alkyl chain is pushed out of the water.

To obtain a fit to the experimental reflectivity data, the electron density $\rho(z)$ of the monolayer was described by a three-layer model.[47,48] The top layer, of thickness L_{alkyl}, represents the close-packed alkyl chains with N_{alkyl} electrons per dimer area, A. The middle layer, of thickness L_{thio}, representing the thiophene dimer has N_{thio} electrons per dimer area, A, and the bottom layer of thickness L_{polar}, representing the solvated polyether chains has N_{polar} electrons per dimer. The resulting step profiles were smeared by a RMS roughness σ, as shown in Figure 5A−D.[47,48] To fit the reflectivity data N_{alkyl}, N_{thio} as well as A (set equal to the area per molecule found from the isotherm) were held constant, while the other parameters were varied for best agreement. After convergence of these parameters, the mean area per molecule (A) was also fitted. The parameters are summarized in Table 4.

5. Transfer to Solid Supports (Langmuir−Blodgett Films). Transfer of monolayers of each of the amphiphilic polymers to

(83) Larsen, N. B.; Bjørnholm, T.; Garnaes, J.; Als-Nielsen, J.; Kjaer, K. *Synth. Met.* **1995**, *71*, 1985−1988.

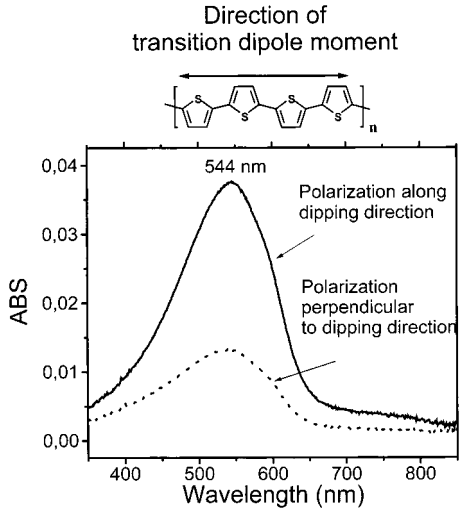

Figure 6. UV−vis absorption spectrum of a glass slide covered on both sides with a monolayer LB film of polymer **1** taken with polarized light. The dichroism shows that the polymer is oriented along the dipping direction during the transfer to solid support by vertical dipping.

a solid hydrophilic support (glass or silicon with an SiO_2 top layer) by the Langmuir−Blodgett technique proceeds with transfer ratios of 1.0 ± 0.1. For a typical example as **1**, visible, magenta-colored Langmuir−Blodgett monolayer films are formed having an anisotropic orientation of the polycrystalline domains, as seen from a dichroic ratio of about 4 observed in the optical absorption spectrum of the films (Figure 6). The largest absorption is along the dipping direction, showing that the transferred films have the polymer backbones oriented primarily along this direction. Within the domains, the polymers are still highly conjugated as indicated by the solid state $\lambda_{max} = 544$ nm of regioregular **1** approaching the highest λ_{max} observed for polythiophene thin films[84,85] (Table 2). As seen by comparisons of **6-RR** and **6-RIR** from Table 2, λ_{max} changes from ~545 to 520 nm when the degree of regioregular head-to-tail couplings changes from 95% to 80%. The reduced order is also expressed in a decrease in crystallinity as evidenced by diffraction (Figure 3B,C).

Figure 7 shows an image of a LB monolayer film obtained from an optical microscope equipped with crossed polarizers. The amorphous glass substrate has a dark-gray color, as shown around **A**. A domain that rotates the light, so more light passes through the top polarizer is shown as **B**, while on the opposite, a dark domain is shown as **C**.

As seen from the size of domain **D**, mm sized, highly oriented monolayer domains can be transferred to glass substrates. Due to the high crystallinity of the Langmuir film, fractures (around arrow **E**) can occur during the transfer to solid supports. Presumably due to the high degree of crystallinity, it has proven difficult, so far, to routinely produce multilayers of the highly regioregular samples by the normal vertical dipping technique.

6. Atomic Force Microscopy of LB Film. In monolayers transferred to hydrophilic silicon substrates by the vertical dipping technique, the polythiophene chains are parallel to the silicon surface with alkyl chains pointing away from the surface as indicated by, e.g., contact angle measurements of the resulting highly hydrophobic surface. Atomic force microscopy of these surfaces reveal flat films (rms roughness = 1.3 Å), which are stable against scanning in contact mode. Due to the disordered state of the protruding alkyl chains, it was not possible to image the in-plane structure of these hydrophobic monolayer surfaces with atomic resolution using AFM.

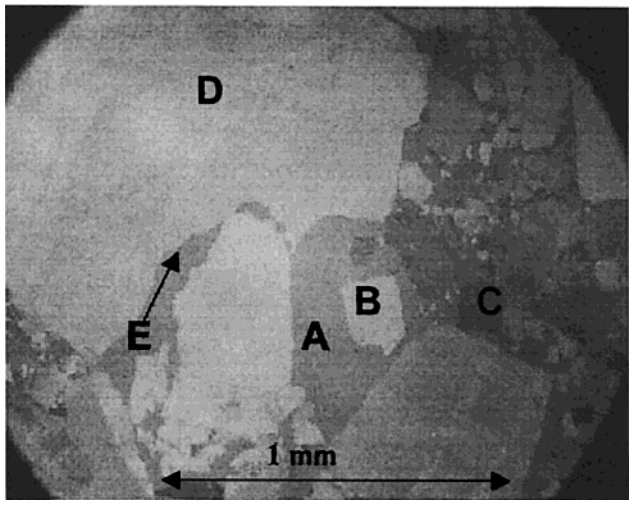

Figure 7. Optical microscope image taken through crossed polarizers of an LB monolayer film at the edge of a large domain. A: The amorphous glass substrate. The angle between the polarizers has been chosen so that the substrate appears dark gray. B: A domain rotating light polarization allowing an increased amount of light to pass through the top polarizer. C: A domain rotating the light in the opposite direction relative to B. D: mm sized monolayer domain rotating the light the same way as B. E: A crack in domain D.

Bilayers consisting of a monolayer of **3** and a monolayer of **4**, or other combinations of the systems described here, can be prepared in two steps: First a hydrophilic silicon wafer is pulled up through the water surface containing a compressed polythiophene monolayer by the standard vertical dipping procedure as described above. Subsequent horizontal dipping of this substrate into the monolayer film allows for alkyl chains sticking out from the LB film surface to hydrophobically assemble with the alkyl chains at the air−water interface resulting in a biomembrane type bilayer with a highly hydrophilic surface (Figure 8, top). Such double layers of, e.g., **4** and **3** transferred to a silicon wafer can be observed by AFM using contact mode (Figure 8, bottom). The smooth gray areas represent the top of the intact double layer (Figure 8A). By applying a large force on the cantilever, a square hole ($1\ \mu m \times 1\ \mu m$) was scraped (Figure 8B). By continuous scanning, the bilayer was disrupted, forming long micellar-like structures (Figure 8C) on the Si substrate (Figure 8D).

7. Reflection−Absorption Infrared Spectroscopy.[86] Reflection−absorption infrared spectroscopy (RAIRS) was used to evaluate the conformational and orientational order of the alkyl chains in the Langmuir−Blodgett deposited monolayers of **1** on gold-coated silicon. The peak position and full width at half-maximum (fwhm) for the asymmetric methyl and methylene stretches were evaluated for two different molecular weight fractions that were purified by SEC (Table 5). The values reported in Table 5 are representative samples for each molecular weight fraction. The monolayers were deposited during the upstroke (hydrophilic tail adsorbing to the surface) onto the gold films. The nature of the surface upon which the polymer films were transferred (i.e., surfaces that were hydrophobic (bare gold) or hydrophilic (mercaptoacetic acid treated gold substrate)) does not appear to affect the order of the films.

(84) McCullough, R. D.; Tristram-Nagle, S.; Williams, S. P.; Lowe, R. D.; Jayaraman M. *J. Am. Chem. Soc.* **1993**, *115*, 4910.

(85) Bjørnholm, T.; Greve, D. R.; Geisler, T.; Petersen, J. C.; Jayaraman, M.; McCullough, R. D. *Adv. Mater.* **1996**, *8*, 920−923.

(86) Ulman, A. *An Introduction to Ultrathin Organic Films. From Langmuir−Blodgett to Self-assembly*; Academic Press: London, 1991.

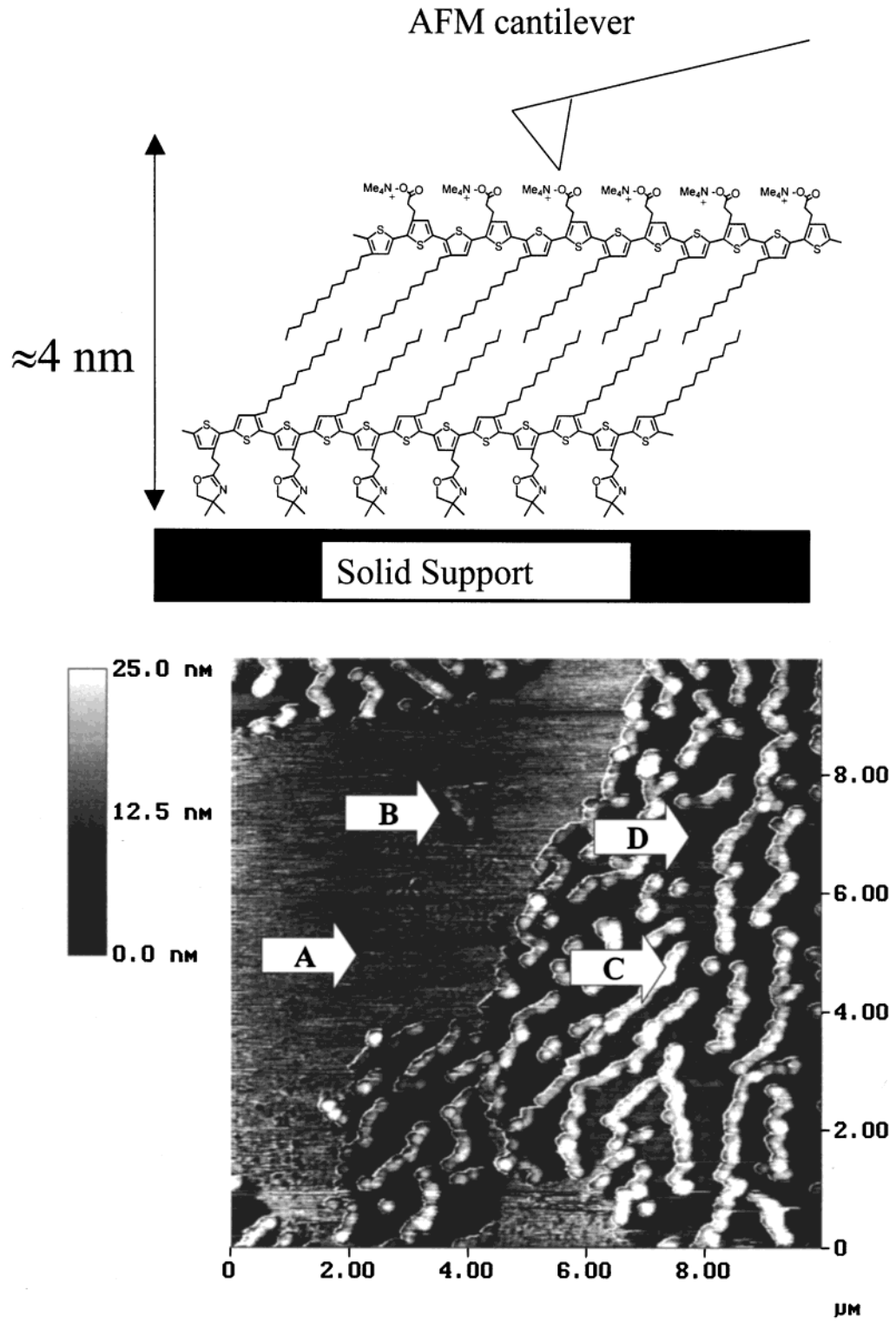

Figure 8. AFM image of a bilayer of polymer **4** and polymer **3** on Si wafer base. Top: schematic illustration of the biomembrane-like double layer being probed by the AFM cantilever in contact mode. Bottom: A: Intact double layer. B: 1 μm × 1 μm hole in the double layer, scraped by application of a large force on the cantilever. C: By continuous scanning, the bilayer was disrupted, forming long micellar-like structures. D: Si solid support.

The orientational and conformational order can be assessed by comparison of the peak position and full width at half-maximum (fwhm) for the IR active $-CH_2-$ and $-CH_3$ modes of the aliphatic side chains in the ordered polymer monolayer films relative to that observed for similar linear hydrocarbon chains. Here, the degree of crystallinity of the monolayer is evaluated by comparing the position of the most intense IR stretching mode, i.e., the CH_2 asymmetric stretch, to the position observed for polyethylene as both a solid with $\nu_{asym}(CH_2) = 2918\ cm^{-1}$ and liquid with $\nu_{asym}(CH_2) = 2924\ cm^{-1}$. The degree of conformational order is also addressed by the fwhm of the asymmetric stretching frequency where values of $14-18\ cm^{-1}$ indicate that the structure does not possess many gauche defects, suggesting the packing motif enforces a close-packed structure

with an all trans arrangement. A much broader peak ~30 cm^{-1} is observed in liquid PE where the C−C bond is free to rotate about the molecular axis.

Large changes in both peak position and fwhm are observed for the two molecular weight fractions of **1**. The larger molecular weight fraction displays a peak position of "liquidlike" alkyl chains in the monolayer, whereas the peak position of the smaller molecular weight fraction appears much more crystalline. The conformational order, likewise, indicates a greater degree of gauche defects in the larger molecular weight fraction. The results suggest that the alkyl chains in the low molecular weight fraction order more readily than the relatively extended backbone of the higher molecular weight fraction that would presumably require more annealing to pack closely. This is in excellent agreement with the GIXD data presented in the preceding sections (Figure 4). In summary, the RAIRS data indicate, that the alkyl chains may have few gauche defects and locally ordered environments. GIXD shows that this order does not extend over many unit cells as evidenced by a measured coherence length from the alkyl chains of ~10 Å.

8. Electrical Conductivity. Four-probe measurements of the electrical conductivity of I_2 or $AuCl_3$ doped monolayers of **1** yield values in excess of 100 S/cm.[42,87] For 100 nm thick spin cast films consisting of locally ordered nano-crystals of regioregular HT coupled poly(3-dodecylthiophene) we measure conductivity values between 500 and 750 S/cm in agreement with previous reports.[84] Conductivity measurements of bundles of nanowires formed by collapsing the monolayer of **1** are slightly lower than those measured for the pure monolayer (~40 S/cm).[43] Details of these data, indicating that the polythiophene Langmuir films presented here possess the highest conductivities measured on a single component Langmuir film to date, are presented elsewhere.[43,87,88]

Summary and Discusson

Using new amphiphilic derivatives of poly(3-alkylthiophene)s, it has been shown that membrane-like Langmuir films, consisting of highly ordered and densely packed domains of the conjugated polymer, can be formed. The domains self-assemble at the air/water interface, and diffraction experiments show that the local structure is held together by favorable intermolecular π-electron interactions. The amphiphilic nature of the molecules allows manipulations thanks to the hydrophobic effect. This has been demonstrated in a preceding publication by replication of an electronic circuit structure through selective transfer of the amphiphilic film to a substrate with the circuit structure pattern printed in the form of hydrophobic and hydrophilic areas, respectively.[42,44]

To obtain a well-defined monolayer of highly ordered domains of polythiophene (as measured by in-plane diffraction on floating monolayers on water), we find that the degree of regioregular head−tail couplings should be as high as possible, the length of the polymer should be considerably longer than 2 thiophene units and shorter than 66, the molecular weight distribution should be as narrow as possible, and the length of the alkyl chain should be less than 17 carbon atoms. Finally, the polymer should be amphiphilic.

The assembly process may be described as consisting of the following steps: (i) the individual macromolecules are organized into floating "boards" on the water surface due to the alternating hydrophilic and hydrophobic substituents on the polymeric core (Figure 9A,B). The long axis of these preorganized objects is confined to the plane of the water surface. (ii) The further assembly of the rigid floating "boards" is effectively a problem similar to ordering matches floating on water. If the individual boards can attract each other through π-stacking they will cluster on the surface in π-stacks. The intermolecular interactions between alkyl chains grafted onto the boards control the relative orientation of adjacent π-stacked boards in the direction perpendicular to the π-stack. In the case of amphiphilic regioregular polythiophene derivatives the void space between alkyl chains on one board will simply be filled by the similarly spaced alkyl chains on the adjacent board by displacing the board by one thiophene unit relative to its neighbor. It can hence be argued that control of a stepwise assembly process of surfactants on the water surface can be achieved by designing surfactants in which π-stacking drives the assembly in one direction while the packing of the alkyl chain locks the structure in the perpendicular (in-plane) direction. Ongoing studies of disklike amphiphiles support this hypothesis.[89]

Serving as a reference to the studies of amphiphilic polythiophenes, studies of the amphiphilic bithiophene derivative (**2**, Table 1, Figure 9A′−F′) shows that this molecule, contrary to the polymeric analogue, cannot organize spontaneously into highly ordered domains, as evidenced by the lack of in-plane order in the resulting films. Two factors seem to induce disorder. The first is the tendency of the molecule to tilt the axis going along the thiophene units (the backbone in the polymer case) out of the plane of the interface when compression occurs. The other is the disorder created in the alkyl chain packing because these are not preorganized in an equidistant way as for the regioregular polymer. In essence the molecule is to small and flexible for predictions to be made about the packing since neither the alkyl chains (which in pure phases do crystallize) nor the π-system is allowed to dominate the packing. In this respect the dimer **2** resembles other small electroactive surfactants in which an electroactive headgroup has been attached to an alkyl chain.[27,33] This observation underlines the importance of confining the amphiphilic molecule in the plane of the water surface in order for the self-assembly mechanism of "alkyl substituted rigid boards", described above, to efficiently lead to ordered domains.

Highly ordered local structures are the prerequisite for obtaining good electronic properties such as high carrier mobility or, in a permanently doped film, high in-plane conductivity. The self-assembly of the amphiphilic polythiophene derivatives presented here offers one possible way of achieving this goal on the nanometer scale as evidenced by the diffraction studies presented, and indeed high conductivities of doped films have been measured ($\sigma \approx 100$ S/cm) on these films.[87] For applications in macroscopic devices the electronic connections at domain boundaries are essential for conduction from one domain to the next. Comparisons of the compressibility of the individual domains in the Langmuir films of polythiophene (measured by diffraction) to the average macroscopic compressibility (measured from the Langmuir isotherm) show that domain boundaries are soft compared to the interior of the domains indicating loss of order at the boundaries. This is not ideal for obtaining a high macroscopic conductivity. Disorder at the domain boundaries is hence the most likely reason for the low value of the conductivity as compared to crystalline samples of conjugated polymers ($\sigma \approx 10.000$ S/cm,[3,4]). Analysis reported elsewhere[43] of the temperature dependence of the conductivity of I_2-doped

(87) Bøgild, P.; Grey, F.; Hassenkam, T.; Greve, D. R.; Bjørnholm, T. *Adv. Mater.***2000**, in press.

(88) Hassenkam, T. Manuscript in preparation.

(89) Reitzel, N.; Hassenkam, T.; Balashev, K.; Jensen, T. R.; Kjaer, K.; Howes, P. B.; Fechtenkötter, A.; Brand, J. D.; Ito, S.; Müllen, K.; Bjørnholm, T. Manuscript in preparation.

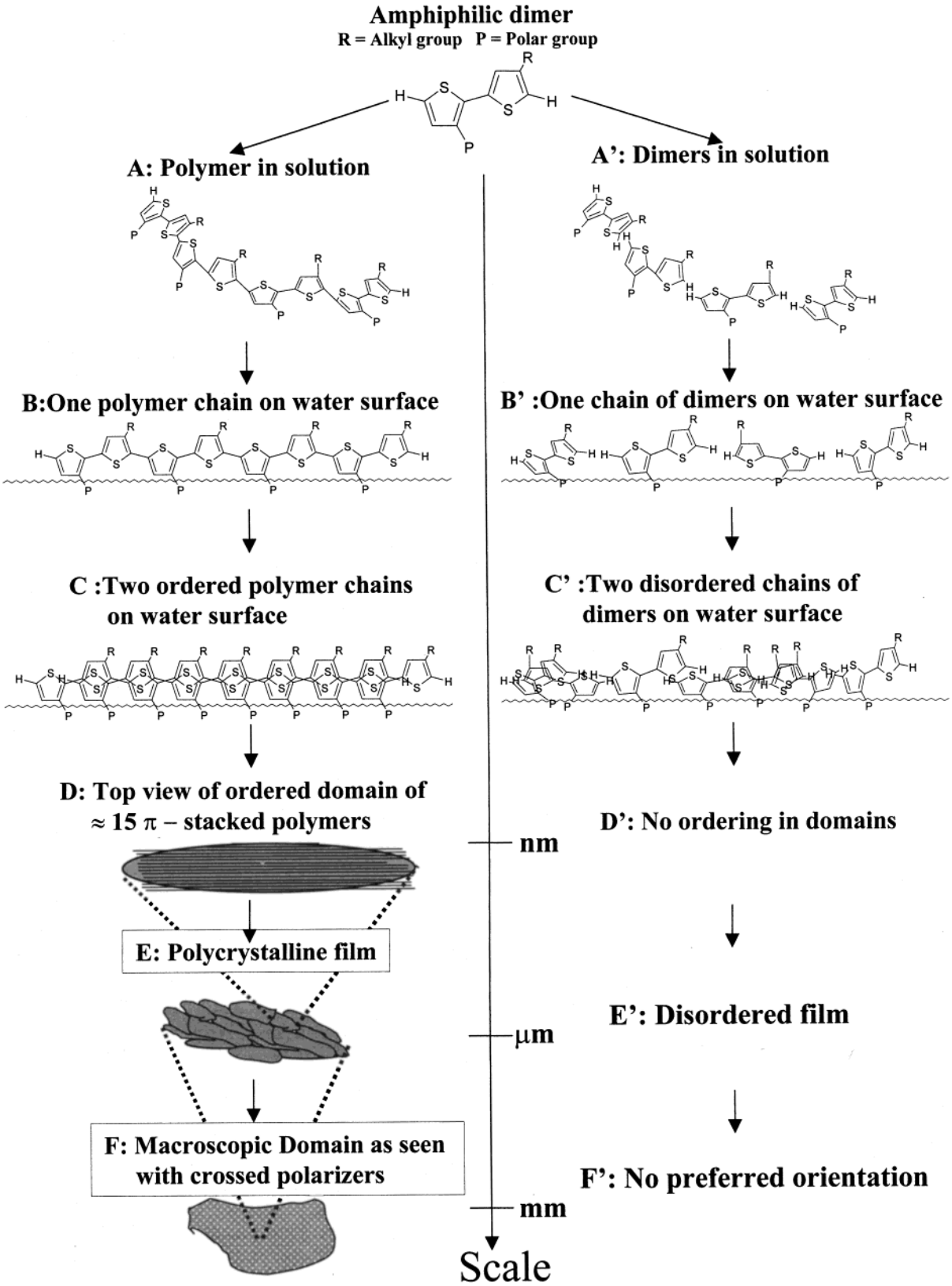

Figure 9. Summary of the steps in the formation of a Langmuir film of amphiphilic polythiophene (left) and the amphiphilic repeat dimer unit (right). By combination of the experimental techniques described in the text, the process has been mapped out all the way from the molecular- to millimeter scale.

polythiophene nanowires prepared by collapse of the Langmuir films discussed here, is in accordance with this model. The analysis indicates that the nanowires consist of highly conducting domains connected through regions of disordered polymers possessing an activated conductivity.[43]

The processability of Langmuir films into multilayer structures is intimately connected to the viscosity of the films which have to flow continuously from the water surface onto the substrate when transferred by the Langmuir−Blodgett technique. In this context crystallinity is a hindrance for efficient transfer

because the films become too brittle. The requirements for processable films is hence in conflict with the requirements for high quality electronic properties (mobility and conductivity). With regard to viscosity the tilted interpenetrating alkyl chains are likely to prevent two adjacent polymers to easily slide against each other. Design of new molecular structures in which this problem is solved may hence be an important step forward toward films with better rheological properties while still retaining a high degree of local order.

Spin cast films of poly(3-alkylthiophens) are presently being developed as the organic constituents in field effect transistors.[58,90−92] For this application the carrier mobility is one of the essential parameters to optimize. The work with field effect transistors therefore has many analogies to the work on optimization of the conductivity in the doped polythiophene films. In both cases the successful optimization will rely on improved understanding and control of the structure of the sample on all scales. Langmuir−Blodgett films will probably not find their way to mass produced organic field effect transistors because they are too complicated to fabricate, but from the assembly point of view they are interesting "2-dimensional" analogues to the three-dimensional cast films. One advantage is that unique structural characterization, both using X-rays and scanning probes, is possible as described above. Furthermore, the morphology of the monomolecular layers is easier to characterize because they are confined to an interface. It is therefore interesting to note that systems in which the assembly is directed by π-stacking organize in the same type of local structure both on the water surface and as bulk films.[42,73,93] The polythiophene samples described above provide one example hereof.

Conclusions

The results presented here on amphiphilic polythiophenes show that it is possible to design a molecule, which allows the coexistence of a fully conjugated and π-stacked polymer structural motif and a membrane forming motif. These results hence open a new road to the organization of highly ordered conjugated systems by way of the "membrane formation" of amphiphilic molecules. In biological systems amphiphiles are known not only to form floating monolayers (Langmuir-films) but also a wealth of other supramolecular structures such as vesicles, and micelles and these may be interesting target structures for future incorporation of a functional π-electron system. Already the amphiphilic nature of the polythiophene thin films discussed here have lead to replication of electronic chip structures by use of the hydrophobic effects[42,44] and to formation of nanowires of polythiophene.[43]

Preparation of conducting or semiconducting thin films of high electronic quality (i.e., high conductivity or carrier mobility respectively) from solutions of conjugated polymers provides a tremendous challenge for the supramolecular chemist. This is because molecules need to be taken fast and efficiently from a disordered state in solution into highly ordered structures in the thin films. As part of this puzzle, the pseudo-2-dimensional self-assembly process at the air−water interface can provide interesting in-sight on how the supramolecular structure can be controlled. In the present paper we have reported the first detailed study on the self-assembly at the air−water interface of an important member for the conjugated polymer family, poly(3-alkylthiophene), and we have shown that considerable insight is now available about the local (angstrom scale) organization of molecules on the surface and in particular about factors controlling the competition between π-stacking and alkyl chain packing.

Acknowledgment. We thank NSF (CHE-9509959), NATO CRG (SRG 941351), the Danish Research Councils (SNF, STVF, MUP, grant nos. 9400892, 9501197, DanSync), and the European Union through TMR-contract ERBFMGECT950059 for financial support of this work and HASYLAB at DESY, Hamburg, for beam time at beam line BW1. We wish to thank Allen J. Bard for use of his Langmuir−Blodgett equipment during T.B.'s sabbatical in Austin.

JA9924501

(90) Bao, Z.; Dodabalapur, A.; Lovinger, A. J. *Appl. Phys. Lett.* **1996**, *69*, 4108.
(91) Dodabalapur, A.; Torsi, L.; Katz, H. E. *Science* **1995**, *268*, 270.
(92) Sirringhaus, H.; Tessler, N.; Friend, R. H. *Science* **1998**, *280*, 1741−1744.
(93) Fell, H. J.; Samuelsen, E. J.; Als-Nielsen, J.; Grübel, G.; Mårdalen, J. *Solid State Commun.* **1995**, *94*, 843−846.
(94) Greve, D. R. Ph.D. Thesis, University of Copenhagen, 1999.